

Chapter 4

Hyperfine shift and relaxation in the presence of chemical exchange

Contents

4.1. Introduction	111
4.2. A pictorial view of chemical exchange	112
4.3. NMR parameters in the presence of exchange	113
4.3.1. Exact solutions for two-site exchange	113
4.3.2. Exchange of excess metal ligands	115
4.3.3. Temperature and exchange	119
4.3.4. Saturation transfer	120
4.4. Equilibrium constants	122
4.4.1. NMR of metal ligands	122
4.4.2. NMR of water protons (the enhancement factor)	123
4.5. Beyond the concept of binding site	125
4.5.1. τ_M as correlation time	125
4.5.2. Outer sphere relaxation	125
4.5.3. Bulk susceptibility shift	127
References	130

4.1. Introduction

If a chemical species containing the investigated nucleus undergoes chemical exchange among different chemical environments, the nuclear NMR parameters are affected in several ways. A full treatment of chemical exchange is rather cumbersome, both from the points of view of shift and of relaxation properties, and is beyond the scope of this book. It is worth noting that even in the simple case of exchange between two sites, the general solution implies non-exponentiality of relaxation. Fortunately, there are some limiting cases which are much easier to treat and for which simple equations can be given. These limiting cases also often hold when one of the chemical environments is paramagnetic.

In general, in the presence of chemical exchange, the nuclei of interest will spend a fraction of time residing in each of n different chemical environments. The probability P_i of finding a chosen nucleus in a particular site i , will be equal to the molar fraction f_i of nuclei in that environment:

$$P_i = f_i = \frac{N_i}{\sum_{i=1}^n N_i} \quad (4.1)$$

where N_i is the number of nuclei in the i th site, $\sum_i N_i$ is the total number of nuclei in the sample, and $\sum_i P_i = 1$ by definition.

Here, the only approximation is to neglect the time spent by a nucleus *in moving* from one environment to another. For example, consider a 0.1 mM water solution of a $\text{Ni}(\text{CH}_3\text{NH}_2)_6^{2+}$ complex, in the presence of 0.1 M excess methylamine, assuming that the complex is fully formed under these conditions. If there is chemical exchange between bound and free methylamine, the methyl protons will spend

$$P_{\text{bound}} = \frac{6 \times 10^{-4}}{10^{-1} + 6 \times 10^{-4}} \approx 6 \times 10^{-3}$$

of the time in the bound position and

$$P_{\text{free}} = \frac{10^{-1}}{10^{-1} + 6 \times 10^{-4}} \approx 1$$

of the time in the bulk solution.

The NH_2 protons can also exchange with water molecules. The probability of finding such a proton in each of the three environments will be

$$P_{\text{bound}} = \frac{6 \times 10^{-4}}{55.5 + 10^{-1} + 6 \times 10^{-4}} \approx 1.1 \times 10^{-5}$$

$$P_{\text{free}} = \frac{10^{-1}}{55.5 + 10^{-1} + 6 \times 10^{-4}} \approx 1.8 \times 10^{-3}$$

$$P_{\text{H}_2\text{O}} = \frac{55.5}{55.5 + 10^{-1} + 6 \times 10^{-4}} \approx 1$$

where 55.5 is the approximate molarity of water. Therefore, the exchangeable protons will only spend about 1/100 000 (i.e. P_{bound}) of their time in a bound position.

The probabilities, or molar fractions, are equal to the fraction of time a nucleus will spend in a particular environment when observed for a suitably long period of time. They do not reveal *how long* the nucleus will stay, on average, in each particular position; in other words, the average lifetime of the nucleus in each environment cannot be calculated from the molar fractions. As will be seen, the chemical lifetime or its reciprocal, the chemical dissociation rate, are crucial parameters governing the influence of chemical exchange on NMR parameters.

4.2. A pictorial view of chemical exchange

Consider, for simplicity, the exchange of nucleus with spin I between two sites, A and B:



Although the dissociation rate constants τ_A^{-1} and τ_B^{-1} are not known, it is known that, at equilibrium, $\tau_A/\tau_B = P_A/P_B$. We will give a full description of the effect of variation of τ_A (and τ_B) on the nuclear NMR parameters and describe the relevant equations involved [1,2].

The nuclei in the A site will resonate at a Larmor precession frequency ω_A , and those in the B site will resonate at a frequency ω_B . Under very slow chemical exchange conditions, two signals will be observed, centered at frequency ω_A and ω_B , with intensities proportional to P_A and P_B respectively. When $P_A = P_B$ the two signals will be of equal intensity and $\tau_A^{-1} = \tau_B^{-1} = \tau_M^{-1}$ (Fig. 4.1(A)(1)). If $R_{2A} = R_{2B}$ the two signals have the same linewidth, given by $R_{2A}/\pi = R_{2B}/\pi$. We will also assume that $R_{1A} = R_{1B}$. When the exchange rate increases, i.e. the lifetime in each chemical environment decreases, the uncertainty principle states that the uncertainty in the energy of the nucleus in each of the two environments must increase. The energy uncertainty is reflected in an increase of signal linewidth. The effect becomes appreciable when τ_M becomes comparable with, or shorter than T_{2A} , T_{2B} . Then the effective T_2 for the signals becomes close to τ_M (Fig. 4.1(A)(2)–(4)). In contrast, T_1 is only affected by the efficiency of coupling of the spin system with the lattice in order to undergo spin transitions. Therefore, if these mechanisms are equal in each environment ($R_{1A} = R_{1B}$), longitudinal relaxation will not be affected by exchange between the two sites.

When the exchange rate is further increased to the point where it is about equal to the difference $\Delta\omega$ in resonance frequency of the two environments, the linewidth is also of the same magnitude. Therefore, the two signals are as broad as their separation and a single broad resonance is observed, extending from ω_A to ω_B (Fig. 4.1(A)(5)).

When the exchange rate becomes faster than $\Delta\omega$, then the single resonance, centered at $(\omega_A + \omega_B)/2$, becomes sharper and sharper. From the NMR point of view, the nuclei are now experiencing an average environment and, as the exchange time decreases further, the linewidth eventually returns to the value of the separate signals in the absence of exchange (Fig. 4.1(A)(6)–(9)).

It has been shown that by increasing τ_M^{-1} the resonance frequency of each signal passes from ω_A or ω_B to the average value $(\omega_A + \omega_B)/2$. Fig. 4.1(B) shows that this transition is not smooth, and that the two signals begin to collapse only for τ_M^{-1} values very close to $\Delta\omega$. The situation $\tau_M^{-1} = \Delta\omega/\sqrt{2}$ (Fig. 4.1(A)(5)) represents signal coalescence, i.e. the borderline between the so-called slow- and fast-exchange regions. Thus, slow- or fast-exchange rates can only be defined with respect to the difference in Larmor frequency $\Delta\omega$, and therefore are dependent on the strength of the external magnetic field.

4.3. NMR parameters in the presence of exchange

4.3.1. Exact solutions for two-site exchange

Having introduced the concept of exchange in a pictorial way, we treat now the more general case of exchange between two sites of different population and different

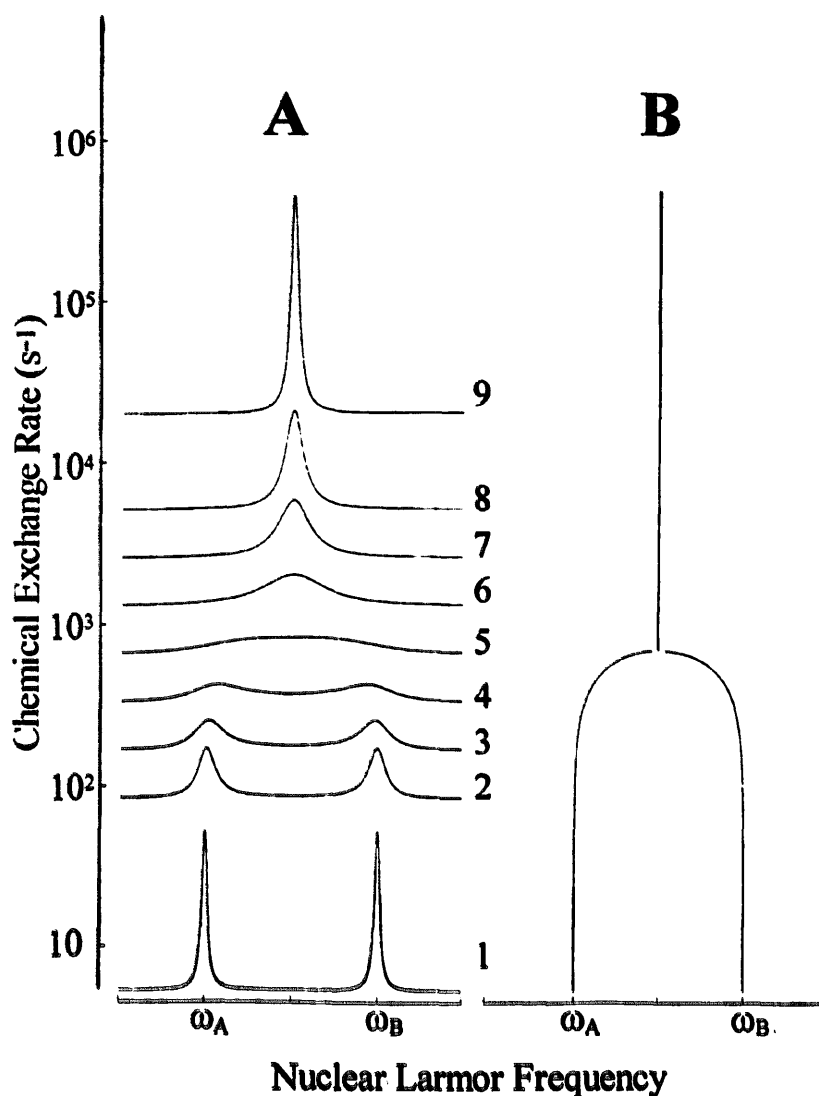


Fig. 4.1. Calculated NMR spectra of a system constituted by a nuclear species in chemical exchange between two sites, A and B, as a function of the chemical exchange rate, τ_M^{-1} (A). The corresponding chemical shift values are shown in (B). The chemical shift separation between the A and B signals is $\Delta\omega = 1000 \text{ rad s}^{-1}$. The various situations are: no exchange (1); slow exchange ((2)–(4)); coalescence (5); fast exchange ((6)–(9)).

intrinsic relaxation times. Under such conditions relaxation is not a single exponential but rather a double exponential process, where the individual rate constants are given by Eqs. (4.2) and (4.3). The chemical shifts are given by Eq. (4.4) [3,4]:

$$R_{1\text{exch}} = A_2 \pm [A_1^2 - (\tau_{1A}^{-1}\tau_{1B}^{-1} - \tau_A^{-1}\tau_B^{-1})]^{1/2} \quad (4.2)$$

$$R_{2\text{exch}} = A_2 \pm \left[\frac{G + (G^2 + H^2)^{1/2}}{2} \right]^{1/2} \quad (4.3)$$

$$\omega_{\text{exch}} = \frac{\omega_A + \omega_B}{2} \pm \left[\frac{-G + (G^2 + H^2)^{1/2}}{2} \right]^{1/2} \quad (4.4)$$

where

$$A_1 = \frac{\tau_{1A}^{-1} + \tau_{1B}^{-1}}{2} \quad A_2 = \frac{\tau_{2A}^{-1} + \tau_{2B}^{-1}}{2}$$

$$G = \frac{(\tau_{2A}^{-1} - \tau_{2B}^{-1})^2}{4} + \tau_A^{-1} \tau_B^{-1} - \frac{\Delta\omega^2}{4}$$

$$H = \frac{\tau_{2A}^{-1} - \tau_{2B}^{-1}}{2} \Delta\omega$$

$$\tau_{1A}^{-1} = R_{1A} + \tau_A^{-1} \quad \tau_{1B}^{-1} = R_{1B} + \tau_B^{-1}$$

$$\tau_{2A}^{-1} = R_{2A} + \tau_A^{-1} \quad \tau_{2B}^{-1} = R_{2B} + \tau_B^{-1}$$

$$\tau_{AB}^{-1} = \tau_A^{-1} + \tau_B^{-1}$$

In the special case of $\tau_A = \tau_B = \tau$, $R_{1A} = R_{1B} = R_1$, and $R_{2A} = R_{2B} = R_2$, the above quantities reduce to:

$$A_1 = R_1 + \tau^{-1} \quad A_2 = R_2 + \tau^{-1}$$

$$G = \tau^{-2} - \Delta\omega^2/4 \quad H = 0$$

and Eqs. (4.2)–(4.4) become

$$R_{1\text{exch}} = R_1 = \text{constant} \quad (4.5)$$

$$R_{2\text{exch}} = R_2 + \tau^{-1} \pm \left(\frac{G + |G|}{2} \right)^{1/2} \quad (4.6)$$

$$\omega_{\text{exch}} = \frac{\omega_A + \omega_B}{2} \pm \left(\frac{-G + |G|}{2} \right)^{1/2} \quad (4.7)$$

Eq. (4.6) accounts for the linewidths of the signals reported in Fig. 4.1(A) and Eq. (4.7) for the chemical shifts reported in Fig. 4.1(B).

4.3.2. Exchange of excess metal ligands

When the paramagnetic site is the least populated, and the difference in population is very large, Eqs. (4.2)–(4.4) can be simplified [3–6]. For example, the chemical shift for the signal in the diamagnetic site evolves as follows as a function of τ_M

$$\Delta\omega_p = \omega_p - \omega_d = \frac{f_M}{\tau_M^2} \frac{\Delta\omega_M}{(R_{2M} + \tau_M^{-1})^2 + (\Delta\omega_M)^2} \quad (4.8)$$

where ω_p is the experimental shift, ω_d is the chemical shift of the diamagnetic site,

and $\Delta\omega_M$ is the difference in chemical shift between the metal site and the diamagnetic site. In turn, the paramagnetic contribution to the shift in the metal site is given by the equations described in Section 2.2. R_{2M} is the transverse nuclear relaxation rate enhancement in the paramagnetic site (Sections 3.4–3.6). The behavior is illustrated in Fig. 4.2. For $\tau_M^{-1} \gg R_{2M}$, $\Delta\omega_M$, Eq. (4.8) becomes

$$\Delta\omega_p = f_M \Delta\omega_M \quad (4.9)$$

i.e. the signal sits at the weighted average position between ω_d and ω_M .

In analogy with the chemical shift, the relaxation rates of the bulk nuclei will be termed R_{1d} and R_{2d} . In the presence of chemical exchange with nuclei in the paramagnetic site, such rates will be enhanced by an amount R_{1p} or R_{2p} , and the measured values will be

$$R_{1\text{meas}} = R_{1d} + R_{1p} \quad R_{2\text{meas}} = R_{2d} + R_{2p}$$

The longitudinal relaxation rate enhancement R_{1p} goes asymptotically from zero to $f_M R_{1M}$ with increasing τ_M^{-1} (Fig. 4.3(A)), according to the following equation:

$$R_{1p} = f_M R_{1M} \frac{\tau_M^{-1}}{R_{1M} + \tau_M^{-1}} = f_M (T_{1M} + \tau_M)^{-1} \quad (4.10)$$

where R_{1M} is the nuclear longitudinal relaxation enhancement in the paramagnetic

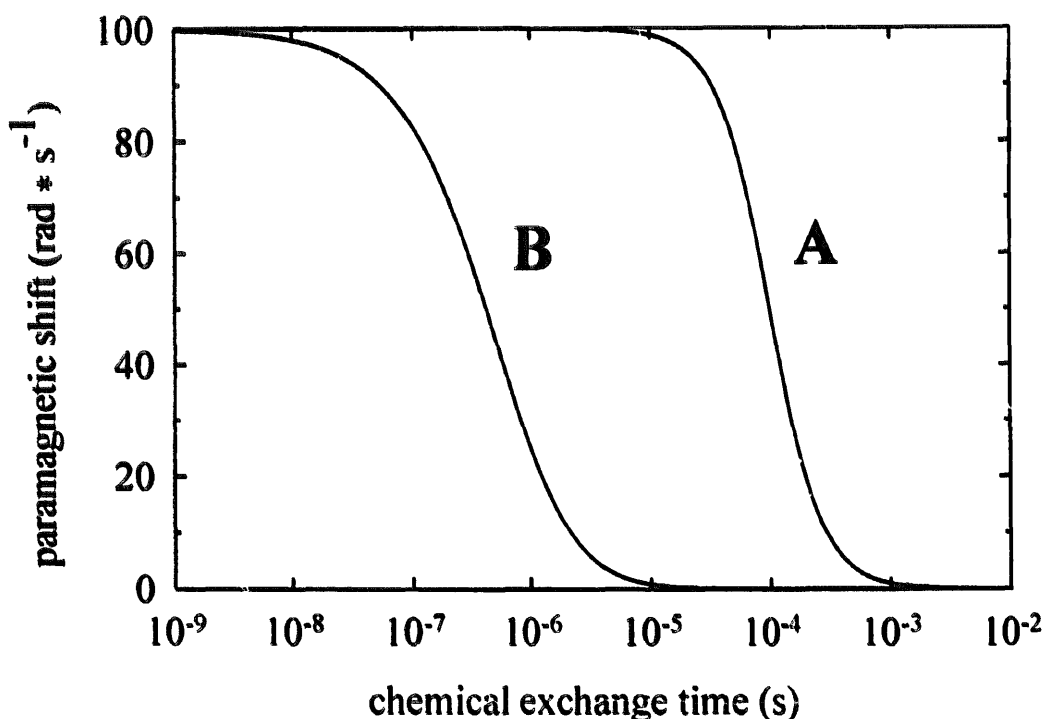


Fig. 4.2. Paramagnetic contribution to the chemical shift $\Delta\omega_p$ as a function of the exchange rate of the nucleus from the paramagnetic site τ_M . Conditions: $\Delta\omega_M = 10^4 \text{ rad s}^{-1}$, $f_M = 10^{-2}$, $R_{2M} = 10^3$ (A) or 10^6 (B) s^{-1} .

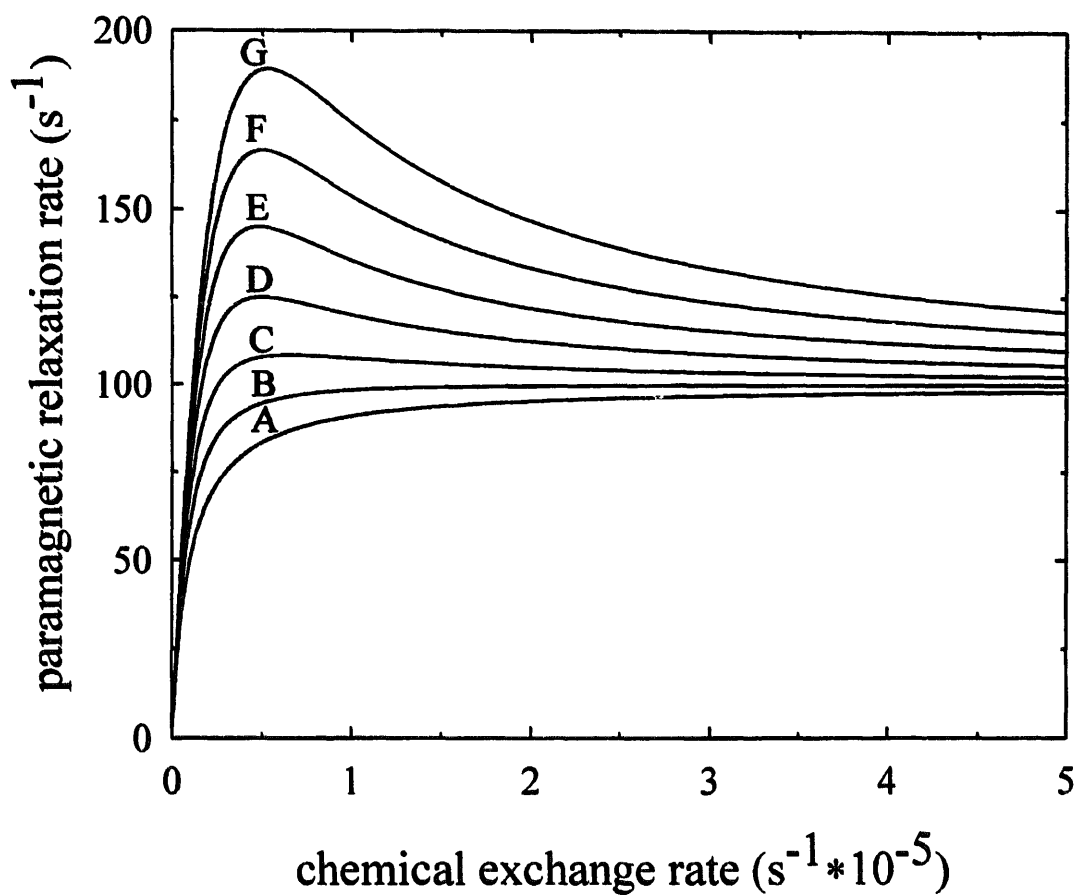


Fig. 4.3. Paramagnetic contributions to the nuclear relaxation rates R_{1p} (A) and R_{2p} (A)–(G) as a function of the exchange rate of the nucleus τ_M^{-1} from the paramagnetic site. Conditions: $R_{1M} = R_{2M} = 10^4 \text{ s}^{-1}$, $f_M = 10^{-2}$, $\Delta\omega_M = 0$ ((A) coincident with R_{1p}), 1×10^{-4} (B), 1.5×10^{-4} (C), 2×10^{-4} (D), 2.5×10^{-4} (E), 3×10^{-4} (F), 3.5×10^{-4} (G) rad s^{-1} .

site (Sections 3.4–3.6). In other words, in the absence of exchange there is no paramagnetic contribution to the relaxation rate of the bulk nuclei, whereas in the fast-exchange limit the measured relaxation rate is the weighted average between the diamagnetic R_{1d} and paramagnetic R_{1M} rates:

$$R_{1\text{meas}} = R_{1d} + f_M R_{1M}$$

where the molar fraction of bound nuclei f_M is the weighting factor. It should be remembered that, as in the case of the paramagnetic shift, R_{1M} can be very large compared with R_{1d} , so that even for small f_M values a noticeable relaxation rate enhancement can be measured.

The transverse relaxation rate enhancement R_{2p} could be treated in the same way if it were not for the difference in chemical shift $\Delta\omega_M$ between the paramagnetic and the diamagnetic species. As has already been shown, the difference in chemical shift causes a line broadening — an increase in R_{2M} — even when the exchange is between two diamagnetic sites. Furthermore, the effect is expected to be much larger in this

case since much larger chemical shift differences are involved. The general formula relating R_{2p} to $\Delta\omega_M$ and τ_M^{-1} of the bulk nuclei is [5,6]

$$R_{2p} = \frac{f_M}{\tau_M} \frac{R_{2M}^2 + R_{2M}\tau_M^{-1} + (\Delta\omega_M)^2}{(R_{2M} + \tau_M^{-1})^2 + (\Delta\omega_M)^2} \quad (4.11)$$

Fig. 4.3 shows the variation of R_{2p} as a function of τ_M^{-1} for different values of $\Delta\omega_M$.

Note that in the absence of exchange ($\tau_M^{-1} = 0$), $R_{2p} = 0$, and for very fast exchange ($\tau_M^{-1} \gg R_{2M}$, $(\Delta\omega_M)^2/R_{2M}$), $R_{2p} = f_M R_{2M}$, as was found for the longitudinal relaxation rate.

In the intermediate region, where τ_M^{-1} is comparable with $\Delta\omega_M$, R_{2p} may be larger than R_{1p} even if $R_{2M} = R_{1M}$ because of exchange broadening effects.

If little or no isotropic shift is present ($\Delta\omega_M \ll R_{2M}$), Eq. (4.11) reduces to

$$R_{2p} = f_M R_{2M} \frac{\tau_M^{-1}}{R_{2M} + \tau_M^{-1}} = f_M (T_{2M} + \tau_M)^{-1} \quad (4.12)$$

which has the same form as that for R_{1p} in Eq. (4.10).

In the very fast exchange regions, the observed paramagnetic effects on the chemical shift $\Delta\omega_p$ and the relaxation rates R_{1p} , R_{2p} , are simply proportional to the full paramagnetic effects in the metal binding site, as summarized below:

$$\Delta\omega_p = f_M \Delta\omega_M \quad R_{1p} = f_M R_{1M} \quad R_{2p} = f_M R_{2M} \quad (4.13)$$

Therefore, if the molar fraction of bound ligand f_M is known, the full paramagnetic effects can be calculated. Of course, if no exchange takes place the ligand in the bulk solution is completely insensitive to the presence of the paramagnetic metal ion.

In the intermediate situation the measured parameters are complicated functions of the full effects experienced in the paramagnetic site ($\Delta\omega_M$, R_{1M} , R_{2M}) and the exchange rate τ_M^{-1} . The τ_M^{-1} dependence of such functions has been summarized in Figs. 4.2 and 4.3. There are, however, particular regions in which the measured parameters are simpler functions of τ_M^{-1} . These regions correspond to cases in which Eqs. (4.8), (4.10) and (4.11) can be approximated by

$$\text{Case I} \quad \Delta\omega_p = \frac{f_M}{\tau_M^2 \Delta\omega_M} \quad (\Delta\omega_M \gg R_{2M}, \tau_M^{-1}) \quad (4.14)$$

Case I occurs when the difference in shift between the paramagnetic and the diamagnetic site, in frequency units, is large compared with both transverse relaxation and the exchange rate. In this case the diamagnetic line is only slightly shifted, and the shift is inversely proportional to the paramagnetic shift.

$$\text{Case II} \quad \Delta\omega_p = \frac{f_M \Delta\omega_M}{\tau_M^2 R_{2M}} \quad (R_{2M} \gg \tau_M^{-1}, \Delta\omega_M) \quad (4.15)$$

Case II occurs when the transverse relaxation rate is faster than both exchange rate and paramagnetic shift. Here the observed shift is directly proportional to the paramagnetic shift.

$$\text{Case III} \quad R_{1p} = f_M \tau_M^{-1} \quad (R_{1M} \gg \tau_M^{-1}) \quad (4.16)$$

$$\text{Case IV} \quad R_{2p} = f_M \tau_M^{-1} \quad (R_{2M} \gg \tau_M^{-1}) \quad (4.17)$$

Cases III and IV represent the slow exchange limits for longitudinal (III) and transverse (IV) relaxation enhancements. The observed enhancements are proportional to the exchange rate, independently of the values of R_{1M} and R_{2M} .

$$\text{Case V} \quad R_{2p} = f_M (\Delta\omega_M)^2 \tau_M \quad (\tau_M^{-1} \gg (\Delta\omega_M)^2 \tau_M \gg R_{2M}) \quad (4.18)$$

Case V is the intermediate exchange case for transverse relaxation. Here, the dependence on τ_M is opposite to that in Case IV. Case V occurs in the presence of relatively large paramagnetic shift, as long as $(\Delta\omega_M)^2$ is small compared with τ_M^{-2} but large compared with $R_{2M} \tau_M^{-1}$.

In Cases III and IV, R_{1p} and R_{2p} are a direct measure of the exchange rate τ_M^{-1} .

4.3.3. Temperature and exchange

The measurement of the exchange time τ_M may provide useful kinetic information on the system. Kinetic parameters for the dissociation process may be obtained by performing relaxation measurements as a function of temperature. If it is assumed that the dissociation of the ligand from the paramagnetic site is a first order kinetic process, the dissociation rate constant τ_M^{-1} is given by the Eyring relationship

$$\tau_M^{-1} = \frac{kT}{h} \exp\left(\frac{-\Delta G^\ddagger}{RT}\right) \quad (4.19)$$

where ΔG^\ddagger is the free energy of activation for the dissociation process.

In the normal range of temperatures used in NMR experiments, the major source of variation of τ_M^{-1} with temperature is contained in the exponential part. In other words, a plot of $\log \tau_M$ against $1/T$ (Arrhenius plot) will give a fairly straight line. Given the linear relationship between τ_M^{-1} and the relaxation rates, straight lines will also be obtained by plotting $\log R_{1p}$ or $\log R_{2p}$ (Cases III and IV) against $1/T$ ($\propto \log \tau_M$) (Fig. 4.4). Note that a straight line of opposite slope is obtained in Case V. The appropriate equations can then be found by simply taking the log of expressions III, IV and V, with τ_M given by Eq. (4.19) (and remembering that $\Delta G = \Delta H - T\Delta S$). From Eqs. (4.16) and (4.17) we thus obtain

$$\log R_{1p} = \log R_{2p} = \log\left(f_M \frac{kT}{h}\right) - \frac{\Delta H^\ddagger}{RT} + \frac{\Delta S^\ddagger}{R} \cong \text{const} - \frac{\Delta H^\ddagger}{RT} \quad (4.20)$$

while from Eq. (4.18) we obtain:

$$\log R_{2p} = \log\left(f_M \Delta\omega_M^2 \frac{h}{kT}\right) + \frac{\Delta H^\ddagger}{RT} - \frac{\Delta S^\ddagger}{R} \cong \text{const}' + \frac{\Delta H^\ddagger}{RT} \quad (4.21)$$

where ΔH^\ddagger and ΔS^\ddagger are the enthalpy and entropy of activation for the dissociation process.

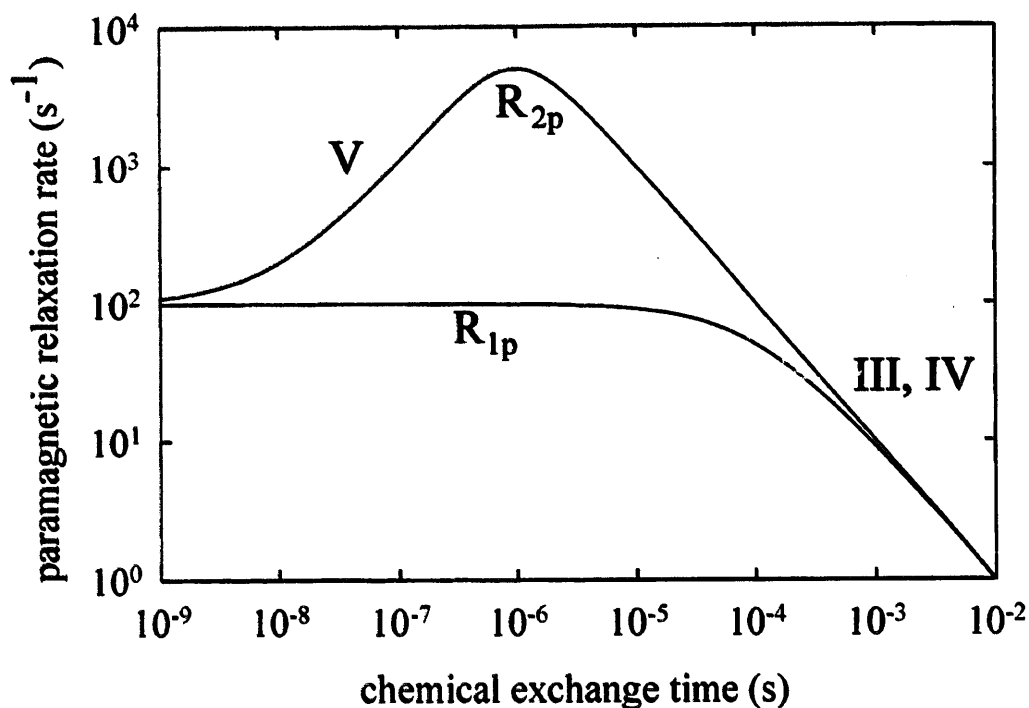


Fig. 4.4. Linear dependence of R_{1p} and R_{2p} (log scale) on τ_M (log scale) in the exchange regions corresponding to Cases III to V. Conditions: $R_M = 10^4 \text{ s}^{-1}$, $f_M = 10^{-2}$, and $A\omega_M = 10^6 \text{ rad s}^{-1}$.

4.3.4. Saturation transfer

As already mentioned (Sections 1.7.4 and 3.13), when a nuclear spin system experiences fluctuating magnetic fields, relaxation occurs. If these fields are produced by other nuclear spins, there is a reciprocal influence that leads to a complicated picture. This will be discussed in detail in Chapter 6. However, if these fluctuating magnetic fields are produced by particles which belong to the lattice, i.e. their energy is negligibly affected by nuclear relaxation (for example, unpaired electrons), the description of the effects is much simpler (Chapter 3) and the return to equilibrium after a perturbation is exponential. Under these circumstances we are going to analyze the effect of chemical exchange.

We have already defined the equilibrium magnetization of a spin I in a given magnetic field B_0 as $M_z(\infty)$, where the (∞) refers to the fact that the sample must have been exposed to the field for a time sufficiently long for equilibrium magnetization to be virtually achieved. After any perturbation from equilibrium of the nuclear spin system such that, at time zero after the perturbation, $M_z(0) \neq M_z(\infty)$, the system will tend to return to equilibrium with a simple rate law of the type

$$\frac{dM_z(t)}{dt} = -R_1[M_z(t) - M_z(\infty)] \quad (4.22)$$

which integrates to an exponential magnetization recovery

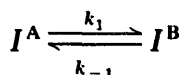
$$M_z(t) - M_z(\infty) = [M_z(0) - M_z(\infty)] \exp(-R_1 t) \quad (4.23)$$

R_1 being the rate constant for the longitudinal relaxation process. In the case of an inversion recovery experiment, $M_z(0) = -M_z(\infty)$, and Eq. (4.23) reduces to

$$M_z(t) = M_z(\infty) - 2M_z(\infty) \exp(-R_1 t) \quad (4.24)$$

which is Eq. (3.30).

The rate equations for a spin system in chemical exchange between two sites



(where $k_1 = \tau_A^{-1}$, $k_{-1} = \tau_B^{-1}$), are given by

$$\begin{aligned} \frac{dM_z^A(t)}{dt} = & -R_1^A [M_z^A(t) - M_z^A(\infty)] - k_1 [M_z^A(t) - M_z^A(\infty)] \\ & + k_{-1} [M_z^B(t) - M_z^B(\infty)] \end{aligned} \quad (4.25)$$

$$\begin{aligned} \frac{dM_z^B(t)}{dt} = & -R_1^B [M_z^B(t) - M_z^B(\infty)] - k_{-1} [M_z^B(t) - M_z^B(\infty)] \\ & + k_1 [M_z^A(t) - M_z^A(\infty)] \end{aligned} \quad (4.26)$$

As anticipated in Section 4.1, solution of these two coupled differential equations gives biexponential behavior, therefore preventing the definition of R_1 for each site (although the two rate constants for the two components are known (Eq. (4.2)). However, Eqs. (4.25) and (4.26) explicitly contain the rate constants for the exchange process, k_1 and k_{-1} , suggesting that they can be used to obtain information on the exchange dynamics through some kind of perturbation on the equilibrium populations of the spins. Suppose that the signal I^A is saturated by applying a weak r.f. on the A resonance for a reasonably long period of time. Then, the steady state intensity of signal B can be obtained from Eq. (4.26) by setting $dM_z^B(t)/dt$ and $M_z^A(t)$ to zero:

$$0 = -(R_1^B + k_{-1}) [M_z^B(t) - M_z^B(\infty)] - k_1 M_z^A(\infty) \quad (4.27)$$

from which we obtain an expression for the fractional change in intensity of signal B upon saturation of A:

$$\frac{M_z^B(t) - M_z^B(\infty)}{M_z^B(\infty)} = \frac{M_z^A(\infty)}{M_z^B(\infty)} \frac{-k_1}{R_1^B + k_{-1}} \quad (4.28)$$

Therefore, by knowing the longitudinal relaxation rate constant of the nucleus in the B site R_1^B in the absence of exchange and by measuring the fractional change in intensity of signal B (called saturation transfer), the rate constants can be obtained. We recall that the two rate constants are related by the fractional populations of the two sites (Section 4.2), in turn proportional to the equilibrium intensities of the two signals:

$$k_1 M_z^A(\infty) = k_{-1} M_z^B(\infty) \quad (4.29)$$

thus, Eq. (4.28) can be further simplified as

$$\frac{M_z^B(t) - M_z^B(\infty)}{M_z^B(\infty)} = \frac{-k_{-1}}{R_1^B + k_{-1}} \quad (4.30)$$

These equations hold for any population distribution of the two sites. Eq. (4.30) is the equation to be used when a saturation transfer experiment is going to be planned.

From the functional form of Eq. (4.30) it is easy to predict the behavior of saturation transfer as a function of the exchange rate. When the rate constant for the $B \rightarrow A$ transformation (k_{-1}) is much smaller than the longitudinal relaxation rate of the nucleus in the B site (R_1^B), the saturation transfer tends to zero. When the rate constant is much higher, the saturation transfer tends to -1 , i.e. there is a total transfer of magnetization to the B site when the A site is kept saturated. Note that these conditions are referred to as fast exchange, even if the exchange is still slow with respect to the chemical shift separation. Fast exchange conditions on the relaxation time scale are often reached before the signals are actually coalesced, so that there is still a reasonable range of exchange rates for which saturation transfer can be observed.

Throughout this section it has been assumed that relaxation in the A and B sites is intrinsically exponential. Warnings about this assumption have been made elsewhere (Sections 3.13 and 6.2.2).

4.4. Equilibrium constants

4.4.1. NMR of metal ligands

Consider a metal complex CM , where C is a multidentate ligand that leaves an empty coordination position on the metal, in the presence of a monodentate ligand L . CM could also be a metalloenzyme interacting with a substrate or an inhibitor L . The paramagnetic effects observed on a nucleus of L can then be used to obtain information on its dissociation constant:

$$K = \frac{[CM][L]}{[CML]} = \frac{(C_{CM} - [CML])(C_L - [CML])}{[CML]} \quad (4.31)$$

where C_{CM} and C_L are the total concentrations of all the metal-containing and ligand-containing species respectively, and $[CML]$ is the equilibrium concentration of the adduct.

Under fast exchange conditions, the molar fraction of bound ligand f_M can be expressed in terms of Eqs. (4.13) and (4.31) as

$$\begin{aligned} f_M &= \frac{[CML]}{C_L} = \frac{\Delta\omega_p}{\Delta\omega_M} = \frac{R_{1p}}{R_{1M}} = \frac{R_{2p}}{R_{2M}} \\ &= \frac{K + C_{CM} + C_L - [(K + C_{CM} + C_L)^2 - 4C_{CM}C_L]^{1/2}}{2C_L} \end{aligned} \quad (4.32)$$

Therefore, measurements of either $\Delta\omega_p$, R_{1p} , or R_{2p} at various concentrations of C_L and/or C_{CM} allow a two-parameter fitting of the data through Eq. (4.32) in terms of K and $\Delta\omega_M$, R_{1M} , or R_{2M} .

If the experimental conditions are such that $[CML]$ is always much smaller than C_L , then Eq. (4.31) becomes

$$K = \frac{(C_{CM} - [CML])C_L}{[CML]} \quad (4.33)$$

and Eq. (4.32) then becomes

$$f_M = \frac{[CML]}{C_L} = \frac{C_{CM}}{K + C_L} \quad (4.34)$$

Expressing f_M in the form of Eq. (4.13) gives

$$C_L = C_{CM} \frac{\Delta\omega_M}{\Delta\omega_p} - K = C_{CM} \frac{R_{1M}}{R_{1p}} - K = C_{CM} \frac{R_{2M}}{R_{2p}} - K \quad (4.35)$$

For constant C_{CM} , a plot of $1/\Delta\omega_p$, $1/R_{1p}$ ($=T_{1p}$), or $1/R_{2p}$ ($=T_{2p}$) against C_L , gives a straight line; $\Delta\omega_M$, R_{1M} , or R_{2M} can then be obtained from the slope, and K can be found from the intercept on the y axis.

Eq. (4.35), like Eq. (4.32), is valid when the ligand is in fast exchange; it is also valid under the exchange-limited conditions, which are described in Eqs. (4.8), (4.10) and (4.11), as long as τ_M is not dependent on C_L . In this case, K can still be obtained, in addition to the limit values of R_{1p} , R_{2p} , or $\Delta\omega_p$ at $f_M = 1$.

4.4.2. NMR of water protons (the enhancement factor)

If one or more ligands L in large excess interact with a metal ion in a metal complex CM in the presence of free metal ions M in solution, then the exchange of ligand L among three sites should be considered. A typical case is when L is a coordinating solvent molecule, e.g. water. The molar fraction of water nuclei is given by

$$f_M = \frac{p[M]}{C_{H_2O}} \quad f_{CM} = \frac{q[CM]}{C_{H_2O}} \quad f_{bulk} = \frac{[H_2O]}{C_{H_2O}} \approx 1 \quad (4.36)$$

where p and q are the numbers of water molecules interacting with free and bound metal ions respectively. The water proton R_{1p} is given by the contribution of the metal, $(R_{1p})_M$, and of the complex $(R_{1p})_{CM}$, both of which can be expressed through Eq. (4.10):

$$\begin{aligned} R_{1p} &= f_M R_{1M} \frac{\tau_M^{-1}}{R_{1M} + \tau_M^{-1}} + f_{CM} R_{1CM} \frac{\tau_{CM}^{-1}}{R_{1CM} + \tau_{CM}^{-1}} \\ &= \frac{p[M]}{C_{H_2O}} R_{1M} \frac{\tau_M^{-1}}{R_{1M} + \tau_M^{-1}} + \frac{q[CM]}{C_{H_2O}} R_{1CM} \frac{\tau_{CM}^{-1}}{R_{1CM} + \tau_{CM}^{-1}} \end{aligned} \quad (4.37)$$

The two limiting cases of the metal completely free ($K \rightarrow \infty$) or completely bound ($K \rightarrow 0$), where K is the dissociation constant of the CM complex, would give

$$\begin{aligned} R_{1p}(\infty) &= \frac{pC_M}{C_{H_2O}} R_{1M} \frac{\tau_M^{-1}}{R_{1M} + \tau_M^{-1}} \\ R_{1p}(0) &= \frac{qC_M}{C_{H_2O}} R_{1CM} \frac{\tau_{CM}^{-1}}{R_{1CM} + \tau_{CM}^{-1}} \end{aligned} \quad (4.38)$$

where C_M is the total metal concentration. The first case can be simulated by simply not adding any ligand C to the solution. It is then customary to define an enhancement factor as [7]

$$\varepsilon = \frac{R_{1p}}{R_{1p}(\infty)} \quad (4.39)$$

where R_{1p} is measured in a solution containing both the metal ion and the ligand C , and $R_{1p}(\infty)$ is obtained from a solution containing the same concentration of metal ion but in the absence of the ligand C . From Eqs. (4.37) and (4.38)

$$\begin{aligned} \varepsilon &= \frac{[M]}{C_M} + \frac{q[CM]}{pC_M} \frac{R_{1CM} \tau_{CM}^{-1}}{R_{1M} \tau_M^{-1}} \frac{R_{1M} + \tau_M^{-1}}{R_{1CM} + \tau_{CM}^{-1}} \\ &= \frac{[M]}{C_M} + \frac{q[CM]}{pC_M} \frac{(T_{1CM} + \tau_{CM})^{-1}}{(T_{1M} + \tau_M)^{-1}} = \frac{[M]}{C_M} + \frac{[CM]}{C_M} \varepsilon_0 \\ &= f_f + f_b \varepsilon_0 = 1 + f_b(\varepsilon_0 - 1) \end{aligned} \quad (4.40)$$

where f_f and f_b are the molar fractions of free and bound metal ion and

$$\varepsilon_0 = \frac{q}{p} \frac{(T_{1CM} + \tau_{CM})^{-1}}{(T_{1M} + \tau_M)^{-1}} = \frac{R_{1p}(0)}{R_{1p}(\infty)}$$

When the CM complex is fully formed, $[M] = 0$ and $[CM] = C_M$; therefore, from Eq. (4.40), $\varepsilon = \varepsilon_0$. ε_0 is thus defined as the enhancement factor measured in a solution where all the metal is complexed. Since usually $q < p$, ε_0 should be smaller than unity if the intrinsic nuclear relaxation times are the same in the metal complex and in the aquaion. However, as often $T_{1CM} < T_{1M}$ owing to a longer correlation time τ_c in the complex (Chapter 3), ε_0 can be larger than unity. This is particularly true when C is a macromolecule (e.g. a protein) and M is a metal ion with long electronic relaxation times.

As it appears in Eq. (4.40), ε_0 is defined only in terms of the molar fraction of bound metal ion; that is, independently of the actual concentrations. By using an equation for f_b analogous to Eq. (4.32), the enhancement factor can be expressed as:

$$\varepsilon = 1 + \frac{K + C_M + C_C - [(K + C_M + C_C)^2 - 4C_M C_C]^{1/2}}{2C_M} (\varepsilon_0 - 1) \quad (4.41)$$

Both K and ε_0 can be obtained through a two-parameter fitting of the ε data obtained at various C_C and/or C_M concentrations.

Eq. (4.41) is valid irrespective of the rate at which water exchanges from the two paramagnetic sites. In fact, the enhancement factor is defined in terms of the quantities $T_{1M} + \tau_M$ and $T_{1CM} + \tau_{CM}$, which are likely to be constant and, in particular, independent of the concentration of the various species in solution. Furthermore, when the exchanging ligand is the solvent, as in the above examples, its concentration is virtually constant under any circumstances.

4.5. Beyond the concept of binding site

4.5.1. τ_M as correlation time

Let us consider a ligand nucleus (e.g. a proton in a water molecule) and its interaction with a paramagnetic center (e.g. a metal ion) to which the ligand is bound. In the absence of exchange, the hyperfine shifts and relaxation rates are given by the equations developed in Chapters 2 and 3. In the case of fast exchange of bulk ligands (e.g. bulk water), we have seen in Section 4.3.2. that the shift and relaxation rates are the weighted averages between the free and bound ligands. This means that *exchange does not alter the shift and relaxing capabilities of the metal site*. Whereas this is always true as far as the shift is concerned, it may not be true for relaxation rates. We have seen that nuclear relaxation in the bound species is proportional to the average squared interaction energy (either dipolar or contact) and to a function of the correlation time that modulates the interaction. We have also seen that the correlation time for the dipolar interaction is given by the reciprocal of the sum of the electronic relaxation rate, the rotational correlation rate, and the chemical exchange rate, whereas in the case of contact relaxation it is given by the reciprocal of the sum of the electronic relaxation rate and the chemical exchange rate (Eqs. (3.5) and (3.6)). We have learned that relaxation arises from the modulation of the interaction energy by whatever random process. If chemical exchange is present, clearly the interaction energy can be modulated by exchange, because the interaction (both dipolar and contact) is lost upon ligand detachment. In the limit situation where τ_M becomes shorter than τ_s (for contact) or shorter than both τ_s and τ_r (for dipolar relaxation) then it becomes the correlation time (Eqs. (3.5) and (3.6)). Of course, the R_{1M} and R_{2M} profiles still maintain the same shape as shown in Figs. 3.10 and 3.12.

4.5.2. Outer sphere relaxation

So far we have assumed that the molecule bearing the nucleus under investigation spends a finite (although small) time in a well-defined binding site, and the rest of the time in the bulk solution at a distance from the metal which may be considered infinite. In this process, we have considered negligible the time spent in approaching and leaving the binding site (i.e. spent at a finite metal–nucleus distance). As τ_M becomes shorter and shorter, it will eventually reach the point where it is comparable with, or shorter than, the diffusional correlation time of the molecule. Under these

conditions, the metal–nucleus interaction during the approach and departure of the ligand becomes a substantial fraction of the total interaction. A limit situation can be reached where a binding site no longer exists and the metal–nucleus interaction is only exerted by random encounters between the molecules, regulated only by diffusion processes. The correlation time for the latter, termed τ_D , then becomes an important parameter. In the only presence of diffusion-controlled interactions, contact shifts no longer exist, and dipolar shifts average to zero if the approach to the ion can occur in every direction. Therefore, hyperfine shifts are zero (although an effect on the shifts can still be detected, see Section 4.5.3), whereas relaxation enhancements do not drop to zero. This situation goes under the name of “outer sphere” relaxation. At variance with the correlation functions encountered so far, the correlation function for molecular diffusion is not exponential [7,8]. Furthermore, its form depends on the assumed diffusional model.

The diffusional correlation time τ_D depends on the size of both the metal and the ligand-containing moieties, according to their diffusion coefficients, D_M and D_L , and on the minimal distance that can be achieved between the ligand and the metal ion, called *distance of closest approach*, d [7,8]:

$$\tau_D = \frac{d^2}{D_M + D_L} \quad (4.42)$$

In turn, the diffusion coefficients are defined by assuming that the molecules behave as rigid spheres in a medium of viscosity η :

$$D_M = \frac{kT}{6\pi a_M \eta} \quad D_L = \frac{kT}{6\pi a_L \eta} \quad (4.43)$$

where a_M and a_L are the radii of the metal-containing and ligand-containing molecules. Note that, when one of the two molecules has a much larger size than the other, its diffusion coefficient is much smaller than the other, and does not contribute appreciably to the denominator of Eq. (4.42). In other words, the diffusional correlation time is only dependent on the size of the small molecule.

In outer sphere relaxation two limiting situations may thus occur, depending on whether the electronic relaxation time τ_s is shorter or longer than the diffusional correlation time τ_D . Since the metal ion and the interacting nucleus are not held together in the same molecular framework, the rotational correlation time τ_r is ineffective in modulating the electron–nucleus interaction and need not be considered further. τ_D is typically in the range 10^{-9} to 10^{-11} s and seldom reaches 10^{-12} s (for instance, water molecules in water have $\tau_D \approx 3 \times 10^{-12}$ s). Thus, τ_s can still be the dominant correlation time when the metal ion undergoes fast electron relaxation. In such a case, one can figure out that, for each metal–ligand distance between d and infinity, the metal–ligand system can be considered as frozen on the time interval over which the electron undergoes many transitions between the spin levels. Therefore, R_{1p} and R_{2p} can be evaluated by simply integrating the Solomon equations

(Eqs. (3.16) and (3.17)) over the distance range between d and infinity [7–9]:

$$R_{1p} = \frac{2}{15} \left(\frac{\mu_0}{4\pi} \right)^2 \frac{N_A [M]}{1000} \frac{4}{3} \pi \frac{\gamma_I^2 g_e^2 \mu_B^2 S(S+1)}{d^3} \left(\frac{7T_{2e}}{1 + \omega_S^2 T_{2e}^2} + \frac{3T_{1e}}{1 + \omega_I^2 T_{1e}^2} \right) \quad (4.44)$$

$$R_{2p} = \frac{1}{15} \left(\frac{\mu_0}{4\pi} \right)^2 \frac{N_A [M]}{1000} \frac{4}{3} \pi \frac{\gamma_I^2 g_e^2 \mu_B^2 S(S+1)}{d^3} \left(4T_{1e} + \frac{13T_{2e}}{1 + \omega_S^2 T_{2e}^2} + \frac{3T_{1e}}{1 + \omega_I^2 T_{1e}^2} \right) \quad (4.45)$$

where N_A is the Avogadro constant and $[M]$ is the concentration of the molecule bearing the paramagnetic center. Note that only the paramagnetic enhancements R_{1p} and R_{2p} can be evaluated, since R_{1M} and R_{2M} cannot be defined. Also, at variance with normal chemical exchange situations, R_{1p} and R_{2p} do not depend on ligand concentration but only on the concentration of the metal-containing species. Indeed, when no binding site exists, each nucleus may interact with more than one metal at a time, independently of the concentration of nuclei; R_{1p} and R_{2p} are therefore only proportional to the number of metal ions per unit volume, which is expressed by $N_A [M]/1000$ in SI units.

In the diffusion-controlled regime different equations should be derived, taking into account that the interaction energy is now modulated by fluctuations in r between d and infinity. In this case the kind of integration to be performed depends on the model assumed for the diffusional behavior of the system. According to one of the most commonly used models for diffusion [10,11], the following equations have been derived when τ_D is the dominant correlation time:

$$R_{1p} = \frac{32}{405} \pi \frac{N_A [M]}{1000} \frac{\gamma_I^2 g_e^2 \mu_B^2 S(S+1)}{d(D_M + D_L)} \{7J(\omega_S) + 3J(\omega_I)\} \quad (4.46)$$

$$R_{2p} = \frac{16}{405} \pi \frac{N_A [M]}{1000} \frac{\gamma_I^2 g_e^2 \mu_B^2 S(S+1)}{d(D_M + D_L)} \{4J(0) + 13J(\omega_S) + 3J(\omega_I)\} \quad (4.47)$$

where the spectral density functions are given by

$$J(\omega) = \frac{1 + 5z/8 + z^2/8}{1 + z + z^2/2 + z^3/6 + 4z^4/81 + z^5/81 + z^6/648} \quad (4.48)$$

with

$$z = (2\omega\tau_D)^{1/2} \quad (4.49)$$

It should be noted that, because the interaction energy is averaged in a different way with respect to the case of shortest τ_s discussed above, the equations look very different. In particular, the $J(\omega)$ do not have the usual Lorentzian form (Fig. 4.5). Equations are also available for the case of τ_D and τ_s having comparable values [12].

4.5.3. Bulk susceptibility shift

In the diffusion limit, the hyperfine shift, defined as the shift difference between a paramagnetic and a diamagnetic environment both measured with respect to the

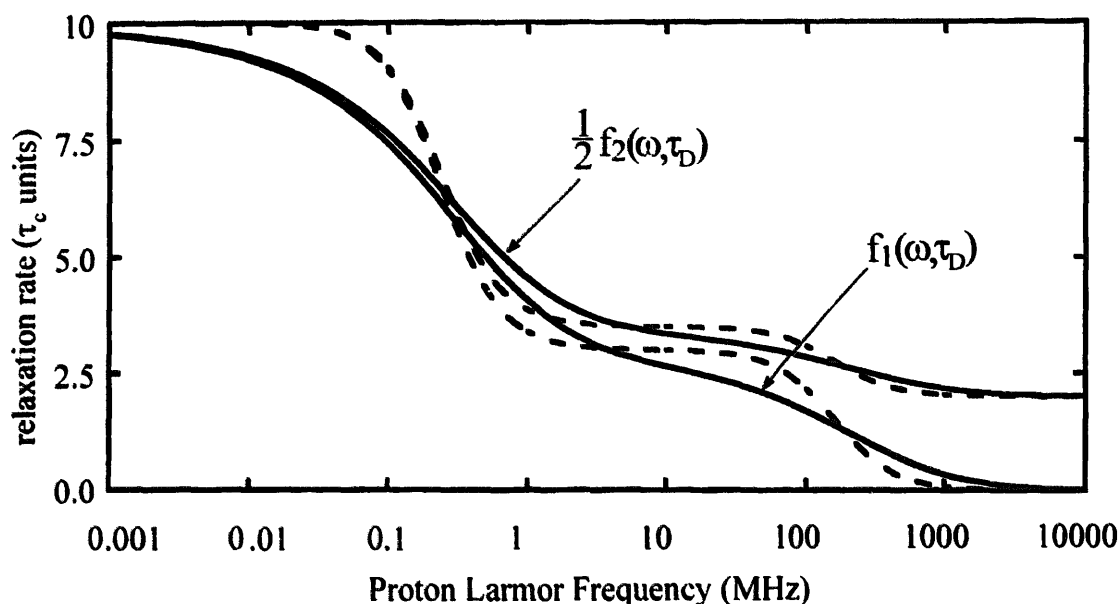


Fig. 4.5. Plot of the spectral density functions of Eqs. (4.41) and (4.42) as a function of magnetic field (expressed as proton Larmor frequency; log scale). $\tau_D = 2 \times 10^{-9}$ s. The Solomon profiles obtained for $\tau_c = 2 \times 10^{-9}$ s are also reported (dashed lines) for comparison purposes.

same internal standard, is zero. However, the absolute shifts of all nuclei in the paramagnetic solution are all offset by the same extent with respect to an analogous diamagnetic solution because of the bulk paramagnetism of the sample. As the effect is the same for all nuclei in the sample, when chemical shifts are reported relative to an internal reference signal the effect is therefore canceled. However, it is possible to measure this effect, which is proportional to the magnetic susceptibility of the paramagnetic solute and to its concentration, by referring the shifts to an *external* reference signal. The experimental procedure is referred to as the Evans method [13], and constitutes one of the best ways of measuring solute magnetic susceptibilities in solution around room temperature.

The contribution to the absolute chemical shift from the magnetic susceptibility of a sample is given by the following equation [14]:

$$\delta_\chi = m \left(\frac{1}{3} - \alpha \right) \left[\chi^{\text{para}} + \chi^{\text{dia}} - \chi^{\text{solv}} \left(1 + \frac{\rho_{\text{solv}} - \rho_{\text{soltn}}}{m} \right) \right] \quad (4.50)$$

where m is the mass of solute per unit volume, α is a demagnetization factor, χ^{para} and χ^{dia} are the paramagnetic and diamagnetic contributions to the mass susceptibility of the solute, χ^{solv} is the mass susceptibility of the solvent, and ρ_{solv} and ρ_{soltn} are the densities of the solvent and the solution respectively. χ^{dia} is negative and usually smaller than χ^{para} in absolute value, unless when dealing with large macromolecules. The demagnetization factor α depends on the geometry of the sample and on its orientation relative to the external magnetic field. For a spherical sample $\alpha = \frac{1}{3}$ and the susceptibility effect on the chemical shift vanishes. For cylindrical samples, $\alpha = \frac{1}{2}$ if the magnetic field is perpendicular to the cylinder's axis (as in most electromagnets)

and $\alpha = 0$ if the magnetic field is parallel to the cylinder axis (as is usual in superconducting magnets). The quantity $\frac{1}{3} - \alpha$ is therefore equal to $-\frac{1}{6}$ in the former case and $\frac{1}{3}$ in the latter; that is, opposite in sign and double in magnitude. Therefore, a high field cryomagnet would be preferable both because of α and higher resolution.

The experimental setup consists of two coaxial tubes (Fig. 4.6) [15], one of which, e.g. the inner one, containing a solution of an inert probe substance and the paramagnetic solute, and the other containing a solution of only the inert probe substance in the same solvent. The shifts of the probe substance differ in the two solutions, and two different signals are observed. Their chemical shift separation is measured, and the experiment repeated with the same solution in the outer tube and a diamagnetic analog in the inner tube. The chemical shift separation of the two signals is again measured. The difference between the two values, if the concentrations of the paramagnetic and diamagnetic solutes are the same, is directly related to χ^{para}

$$\Delta\delta = m \left(\frac{1}{3} - \alpha \right) \chi^{\text{para}} \quad (4.51)$$

Note that the terms containing the solvent susceptibility in Eq. (4.50) cancel because the two solutions have the same density. Eq. (4.51) can also be rewritten as

$$\Delta\delta = 1000M \left(\frac{1}{3} - \alpha \right) \chi_M^{\text{para}} \quad (4.52)$$

where $1000M$ is the concentration (mol m^{-3}) of the paramagnetic solute and χ_M^{para} is the paramagnetic contribution to the molar susceptibility, which is directly related

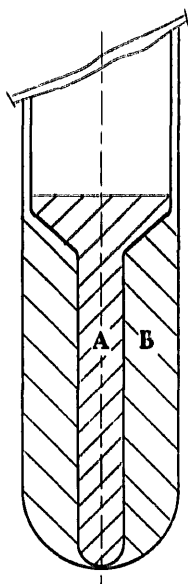


Fig. 4.6. Coaxial NMR tubes for the measurement of magnetic susceptibility of a paramagnetic solute. Solution A contains the paramagnetic solute and an inert probe substance. Solution B contains the probe substance in the same solvent. The measurement is then repeated substituting the paramagnetic solute in A with a diamagnetic analog of the same concentration.

to the effective magnetic moment of the paramagnetic center (Chapter 1):

$$\mu_{\text{eff}}^2 = \frac{3kT}{N_A\mu_0} \chi_M^{\text{para}} \quad (4.53)$$

Typical values of χ_M^{para} range from 2×10^{-8} to $3 \times 10^{-7} \text{ m}^3 \text{ mol}^{-1}$, so that for a millimolar solution in a superconducting magnet ($1000M = 1$, $\alpha = 0$), $\Delta\delta$ goes from 0.007 to 0.1 ppm, that is from 5 to 75 Hz on a 750 MHz instrument.

Possible sources of error may arise if the probe is not completely inert. In fact, even a very weak interaction of the probe with the paramagnetic center may cause specific effects on the chemical shift, which may substantially alter the measurement, given the relatively small effects being measured. The best approach is to repeat the measurements using different probes. Another source of error, for very large macromolecules, lies in the sizable χ^{dia} term, whose absolute value may be of the same order of magnitude or even larger than χ^{para} , making the subtraction more critical.

References

- [1] H.S. Gutowsky, D.M. McCall and C.P. Slichter, *J. Chem. Phys.*, 21 (1953) 279.
- [2] H.S. Gutowsky and C.H. Holm, *J. Chem. Phys.*, 25 (1956) 1228.
- [3] A.C. McLaughlin and J.S. Leigh, Jr., *J. Magn. Reson.*, 9 (1973) 296.
- [4] J.S. Leigh, *J. Magn. Reson.*, 4 (1971) 308.
- [5] T.J. Swift and R.E. Connick, *J. Chem. Phys.*, 37 (1962) 307.
- [6] T.J. Swift, in G.N. La Mar, W.DeW. Horrocks, Jr. and R.H. Holm (Eds.), *NMR of Paramagnetic Molecules*, Academic Press, New York, 1973, pp. 53–83.
- [7] R.A. Dwek, *Nuclear Magnetic Resonance in Biochemistry: Applications to Enzyme Systems*, Oxford University Press, London, 1973.
- [8] A. Abragam, *The Principles of Nuclear Magnetism*, Oxford University Press, Oxford, 1961.
- [9] Z. Luz and S. Meiboom, *J. Chem. Phys.*, 40 (1964) 2686.
- [10] L.P. Hwang and J.H. Freed, *J. Chem. Phys.*, 63 (1975) 4017.
- [11] C.F. Polnaszek, and R.G. Bryant, *J. Chem. Phys.*, 68 (1978) 4034.
- [12] J.H. Freed, *J. Chem. Phys.*, 68 (1978) 4034.
- [13] D.F. Evans, *J. Chem. Soc.*, (1959) 2003.
- [14] W.C. Dickinson, *Phys. Rev.*, 81 (1951) 717.
- [15] W.D. Phillips and M. Poe, *Methods Enzymol.*, 24 (1972) 304.